



Providing Choice & Value

Generic CT and MRI Contrast Agents



CONTACT REP

AJNR


This information is current as
of July 16, 2025.

**Improved Blood Suppression of
Motion-Sensitized Driven Equilibrium in
High-Resolution Whole-Brain Vessel Wall
Imaging: Comparison of Contrast-Enhanced
3D T1-Weighted FSE with Motion-Sensitized
Driven Equilibrium and Delay Alternating
with Nutation for Tailored Excitation**

D.J. Kim, H.-J. Lee, J. Baik, M.J. Hwang, M. Miyoshi and
Y. Kang

AJNR Am J Neuroradiol published online 20 October 2022
<http://www.ajnr.org/content/early/2022/10/20/ajnr.A7678>

Improved Blood Suppression of Motion-Sensitized Driven Equilibrium in High-Resolution Whole-Brain Vessel Wall Imaging: Comparison of Contrast-Enhanced 3D T1-Weighted FSE with Motion-Sensitized Driven Equilibrium and Delay Alternating with Nutation for Tailored Excitation

 D.J. Kim,  H.-J. Lee,  J. Baik,  M.J. Hwang,  M. Miyoshi, and  Y. Kang



ABSTRACT

BACKGROUND AND PURPOSE: High-resolution vessel wall MR imaging is prone to slow-flow artifacts, particularly when gadolinium shortens the T1 relaxation time of blood. This study aimed to determine the optimal preparation pulses for contrast-enhanced high-resolution vessel wall MR imaging.

MATERIALS AND METHODS: Fifty patients who underwent both motion-sensitized driven equilibrium and delay alternating with nutation for tailored excitation (DANTE) preparation pulses with contrast-enhanced 3D-T1-FSE were retrospectively included. Qualitative analysis was performed using a 4-grade visual scoring system for black-blood performance in the small-sized intracranial vessels, overall image quality, severity of artifacts, and the degree of blood suppression in all cortical veins as well as transverse sinuses. Quantitative analysis of the M1 segment of the MCA was also performed.

RESULTS: The qualitative analysis revealed that motion-sensitized driven equilibrium demonstrated a significantly higher black-blood score than DANTE in contrast-enhanced 3D-T1-FSE of the A3 segment (3.90 versus 3.58, $P < .001$); M3 (3.72 versus 3.26, $P = .004$); P2 to P3 (3.86 versus 3.64, $P = .017$); the internal cerebral vein (3.72 versus 2.32, $P < .001$); and overall cortical veins (3.30 versus 2.74, $P < .001$); and transverse sinuses (2.82 versus 2.38, $P < .001$). SNR_{lumen} , contrast-to-noise ratio_{wall-lumen}, and SNR_{wall} in the M1 vessel were not significantly different between the 2 preparation pulses (all, $P > .05$).

CONCLUSIONS: Motion-sensitized driven equilibrium demonstrated improved blood suppression on contrast-enhanced 3D-T1-FSE in the small intracranial arteries and veins compared with DANTE. Motion-sensitized driven equilibrium is a useful preparation pulse for high-resolution vessel wall MR imaging to decrease venous contamination and suppress slow-flow artifacts when using contrast enhancement.

ABBREVIATIONS: BB = black-blood; CE = contrast-enhanced; CNR = contrast-to-noise ratio; DANTE = delay alternating with nutation for tailored excitation; HR-VWI = high-resolution vessel wall MR imaging; ICV = internal cerebral vein; MSDE = motion-sensitized driven equilibrium

High-resolution vessel wall MR imaging (HR-VWI) is a crucial technique used to diagnose various pathologic conditions that involve the vessel walls.¹⁻⁵ HR-VWI differs from conventional methods such as CTA, MRA, and DSA in that HR-VWI directly delineates the vessel walls rather than indirectly illustrating them

by projecting the luminal cavity.^{6,7} Thus, HR-VWI enables further characterization of minute changes in the vessel wall.^{2,5,8-10}


In HR-VWI, suppression of signals from the intraluminal blood and extraluminal CSF is required to precisely portray the vessel wall.^{2,11,12} The 3D-T1-FSE sequence is widely used for HR-VWI due to its inherent black-blood (BB) effect attained by intravoxel dephasing induced by gradient moments and stimulated echoes.^{12,13} However, there are technical challenges associated with HR-VWI, including slow-flow artifacts induced by intraluminal blood with slow-flow velocity, which may mimic vessel wall lesions, particularly when using contrast enhancement in which gadolinium shortens the T1 relaxation times of blood. These technical challenges are difficult to overcome if only the inherent BB effect of 3D-T1-FSE is used.⁵

Received May 12, 2022; accepted after revision September 15.

From the Department of Radiology (D.J.K., H.-J.L., J.B., Y.K.), Haeundae Paik Hospital, Inje University College of Medicine, Busan, South Korea; Department of Radiology (J.B.), Good Gang-An Hospital, Busan, South Korea; GE Healthcare Korea (M.J.H.), Seoul, South Korea; and GE Healthcare Japan (M.M.), Tokyo, Japan.

Please address correspondence to Yeonah Kang, MD, Department of Radiology, Haeundae Paik Hospital, Inje University College of Medicine, Busan, South Korea; e-mail: bsb2312@gmail.com

 Indicates open access to non-subscribers at www.ajnr.org

 Indicates article with online supplemental data.

<http://dx.doi.org/10.3174/ajnr.A7678>

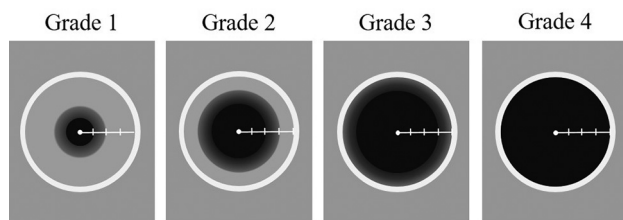


FIG 1. Schematic illustration of vessels with different visual grade scores for BB performance: 1) less than one-half of the target lumen dimension visible with black signal intensity; 2) one-half to three-quarters of the target lumen dimension visible with black signal intensity; 3) more than three-quarters of the target lumen dimension visible with black signal intensity (with unsuppressed flow near the wall); and 4) completely suppressed flow (with the entire target lumen dimension visible with black signal intensity).

Management of these technical pitfalls is necessary because the contrast-enhanced (CE) sequence gives essential clinical information on vasculopathy. The plaque enhancement can be used as a measure of the vulnerability of atherosclerotic plaques.^{4,5,9} Abnormal vessel wall enhancement indicates inflammatory activity, and the degree of enhancement may be reduced after steroid therapy.^{4,5,9} However, incomplete blood flow suppression may mimic atherosclerotic plaque enhancement or vessel wall enhancement.⁵ Hence, additional preparation pulses for HR-VWI such as motion-sensitized driven equilibrium (MSDE) and delay alternating with nutation for tailored excitation (DANTE) have been developed to minimize the degradation of the BB effect and are currently used in various clinical scenarios.^{11,14-19}

To date, effort has been made to find an optimal method for increasing the BB effect in HR-VWI.^{3,13,14,17} Recently, an increased number of studies reported that DANTE has advantages in intracranial application in terms of the provision of effective CSF suppression over MSDE, which has signal drop owing to inherent T2 decay.²⁰⁻²² However, regarding CE situations, we speculated that because MSDE has the characteristics of T2 preparation pulses with a motion-sensitized gradient, fast T1 recovery of the contrast agent may not influence the flow suppression of MSDE. Nevertheless, comparisons between MSDE and DANTE in HR-VWI using CE 3D-T1-FSE have not yet been reported. Therefore, we compared the BB effect of MSDE and DANTE in CE 3D-T1-FSE, particularly in small vessels with slow intraluminal blood flow.

MATERIALS AND METHODS

Patient Selection

The institutional review board of Inje University of Haeundae Paik Hospital approved this study, and the requirement for informed consent was waived due to its retrospective nature. Seventy-one consecutive patients who underwent HR-VWI between January and July 2020 were retrospectively enrolled. Patients who underwent CE 3D-T1-FSE with only 1 BB technique ($n = 19$) or those with poor image quality due to severe motion artifacts ($n = 2$) were excluded. Finally, 50 patients (mean age, 65.6 years; range, 33–87 years) were included in the study.

MR Imaging Protocol

All MR images were acquired using a single 3T MR imaging unit (Signa Architect; GE Healthcare) with a 48-channel head coil.

Examinations were performed 5 minutes after intravenous administration of gadobutrol (Gadovist; Bayer Schering Pharma) at a dose of 0.1 mmol/kg of body weight.⁵ We used identical imaging parameters (TR, 800 ms; echo-train length, 48; bandwidth, 416 Hz/pixel; matrix, 300×300 pixels; FOV, 180×180 mm²; voxel size, $0.6 \times 0.6 \times 0.6$ mm³; 11.7-cm coverage on the coronal plane; compressed sensing factor, 1.2; Autocalibrating reconstruction for Cartesian imaging (ARC) acceleration, phase $\times 2$ and section $\times 1$; acquisition time, 5 minutes 8 seconds with fat saturation) for all the patients. The TE was set to the minimum value; consequently, the TEs were 28 and 17 ms for the MSDE and DANTE scans, respectively. Images of CE 3D-T1-FSE with MSDE (composite-type MSDE; velocity-suppressed target, 3.0 cm/s) and those with the DANTE (flip angle, 13°; Gxyz = 18 mT/m; echo space, 1500 μ s; total duration of the DANTE pulse, 142 ms) were acquired in a randomized order. Among the 50 patients finally included, 26 had images of CE 3D-T1-FSE with DANTE acquired before MSDE, while 24 had images of CE 3D-T1-FSE with MSDE acquired before DANTE.

Image Analysis

Qualitative and quantitative analyses of the BB effects of MSDE and DANTE were performed by 2 radiologists (Y.K. and H.-J.L. with 8 and 13 years' experience in neuroradiology, respectively), blinded to patient clinical information. Qualitative analysis was performed in the M1 segment of the MCA and 4 parts of the small intracranial vessels: the A3 segment of the anterior cerebral artery (A3), M3 segment of middle cerebral artery (M3), from P2 to P3 segment of posterior cerebral artery (P2 to P3), and internal cerebral vein (ICV). For the qualitative analysis, a 4-grade visual scoring system was used and defined as follows: 1) less than one-half of the target lumen dimension visible with black signal intensity; 2) one-half to three-quarters of the target lumen dimension visible with black signal intensity; 3) more than three-quarters of the target lumen dimension visible with black signal intensity (with unsuppressed flow near the wall); and 4) completely suppressed flow (with the entire target lumen dimension visible with black signal intensity). Figure 1 shows the schematic illustration of vessels with different visual grade scores for BB performances. For quantitative analysis, the SNR and contrast-to-noise ratio (CNR) were measured in the same area of the M1 segment of the MCA and calculated according to an equation used in a previous work by Xie et al.¹⁶ $SNR_x = 0.695 \times S_x / \sigma$, $CNR_{x \rightarrow y} = 0.695 \times (S_x - S_y) / \sigma$; S_x represents the signal intensity of x anatomy, and the noise level (σ) was defined as the signal SD within an ROI drawn in the adjacent air space of the image uncontaminated by artifacts. The SNR_{wall} , SNR_{lumen} , SNR_{csf} , $CNR_{wall-lumen}$, and $CNR_{wall-csf}$ were calculated. The sizes of each drawn ROI of the vessel wall and the vessel lumen during quantitative analysis were also recorded. The Online Supplemental Data show an example of SNR measurement with a displayed ROI. All analyses were repeated by another radiologist (J.B., with 7 years' experience in neuroradiology) for the evaluation of interobserver reliability for the BB effect.

Grading of overall image quality, severity of artifacts, and the degree of blood suppression in all cortical veins and both sides of the transverse sinuses was rated in each individual CE 3D-T1-FSE with DANTE or MSDE by 2 reviewers in a blinded manner, and consensus was reached. Each rater evaluated the overall image quality using a 4-grade scoring system as follows: 1) nondiagnostic

Table 1: Visual scoring evaluation of the BB effect in the small-sized intracranial arteries, ICV, and the M1 segment of the MCA

Locations	3D-T1-FSE with MSDE	3D-T1-FSE with DANTE	P Value
A3	3.90	3.58	<.001
M3	3.72	3.26	.004
P2 to P3	3.86	3.64	.017
ICV	3.72	2.32	.001
M1	3.66	3.60	.497

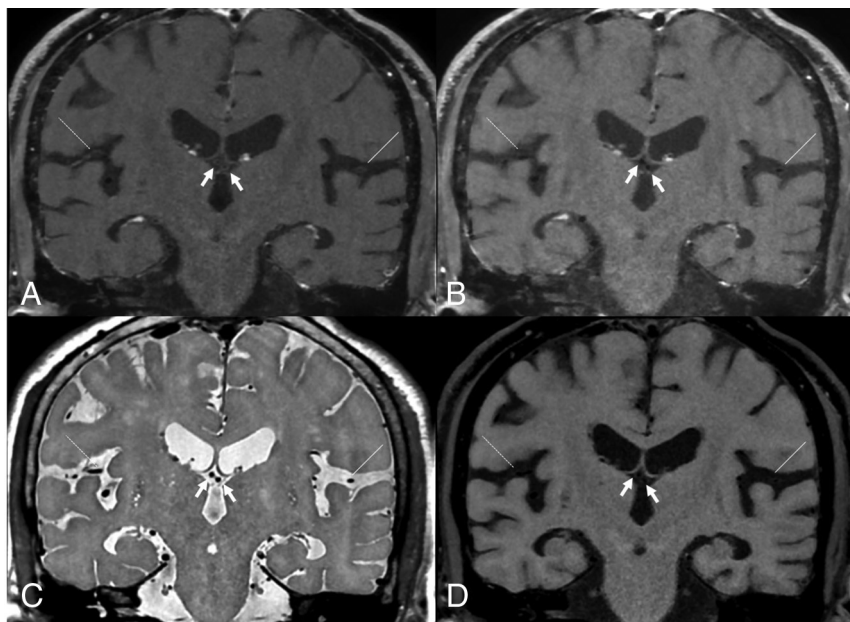


FIG 2. A 78-year-old man who underwent HR-VWI. CE 3D-T1-FSE with DANTE (A), CE 3D-T1-FSE with MSDE (B), a proton-density-weighted sequence (C), and a T1-weighted sequence (D). There are nonsuppressed peripheral flows at the ICV (arrows), cortical vein (dotted line), and left M3 (solid line) on CE 3D-T1-FSE with DANTE (A). However, CE 3D-T1-FSE with MSDE (B) shows complete blood suppression at the aforementioned structures.

image quality; 2) moderately diminished image quality, affecting general diagnosis; 3) minimally diminished image quality, not affecting general diagnosis; and 4) optimal image quality. The severity of artifacts was evaluated using the following 4-grade scoring system: 1) presence of any artifact that inhibits diagnosis of the targeted vessel anatomy; 2) existence of artifacts that affect the targeted vessel anatomy, but still interpretable; 3) existence of artifacts that do not affect the diagnosis of the targeted vessel anatomy; and 4) no artifacts at all. The overall cortical vein suppression score was evaluated using the following 4-grade scoring system: 1) severe nonsuppressed cortical veins that mimic pathology; 2) moderate nonsuppressed cortical veins that do not mimic pathology; 3) mild nonsuppressed cortical veins that do not interfere with interpretation; and 4) complete blood suppression in the cortical veins. The degree of blood suppression on both sides of the transverse sinuses was evaluated using the following 4-grade scoring system: 1) severe nonsuppressed transverse sinuses that mimic pathology; 2) moderate nonsuppressed transverse sinuses with central nonsuppressed blood signals; 3) mild nonsuppressed transverse sinuses with only peripheral nonsuppressed blood signals; and 4) complete blood suppression in the transverse sinuses.

Statistical Analysis

All statistical analyses were performed using R software for Windows (Version 3.3.3; <http://www.r-project.org/>). The normality test for each variable was performed using the Kolmogorov-Smirnov test. Either a paired *t* test or Wilcoxon signed-rank test was performed for comparison. The weighted κ and intra-class correlation coefficients were used to evaluate the interobserver agreement. Statistical significance was set at $P < .05$. The strength of the interobserver agreement was categorized as follows: κ values and intraclass correlation coefficients < 0.20 , poor agreement; 0.21–0.40, fair agreement; 0.41–0.60, moderate agreement; 0.61–0.80, good agreement; and 0.81–1.00, excellent agreement.²³

RESULTS

Qualitative Analysis

CE 3D-T1-FSE with MSDE had a significantly higher visual score than 3D-T1-FSE with DANTE in the small-sized vessels: A3 (3.90 versus 3.58, $P < .001$); M3 (3.72 versus 3.26, $P = .004$); P2 to P3 (3.86 versus 3.64, $P = .017$); and the ICV (3.72 versus 2.32, $P < .001$) (Table 1). In the M1, the qualitative analysis of CE 3D-T1-FSE with MSDE and with DANTE showed no significant difference between the two (3.66 versus 3.60, $P = .497$). Figures 2 and 3 and the

Online Supplemental Data illustrate representative cases in which the BB effect of CE 3D-T1-FSE with MSDE surpassed that with DANTE. Subgroup analysis results of the BB effect according to the scan order are provided in the Online Supplemental Data.

Quantitative Analysis

There were no significant differences in SNR_{lumen} , $CNR_{wall-lumen}$, and SNR_{wall} between CE 3D-T1-FSE with MSDE and with DANTE in the M1 (all, $P > .05$) (Table 2). However, $CNR_{wall-csf}$ was higher on 3D-T1-FSE with DANTE than with MSDE (1.785 versus 1.047; $P = .013$). The mean sizes of the drawn ROI of the vessel wall and the vessel lumen were approximately 0.0037 cm² and 0.0437 cm², respectively.

Interobserver Reliability

The interobserver reliability evaluation indicated good agreement in both qualitative (0.78; 95% CI, 0.69–0.86) and quantitative (0.71; 95% CI, 0.63–0.77) analyses (Online Supplemental Data).

Image-Quality Assessment

CE 3D-T1-FSE with DANTE was rated slightly higher than with MSDE for overall image quality (3.54 versus 3.42, $P =$

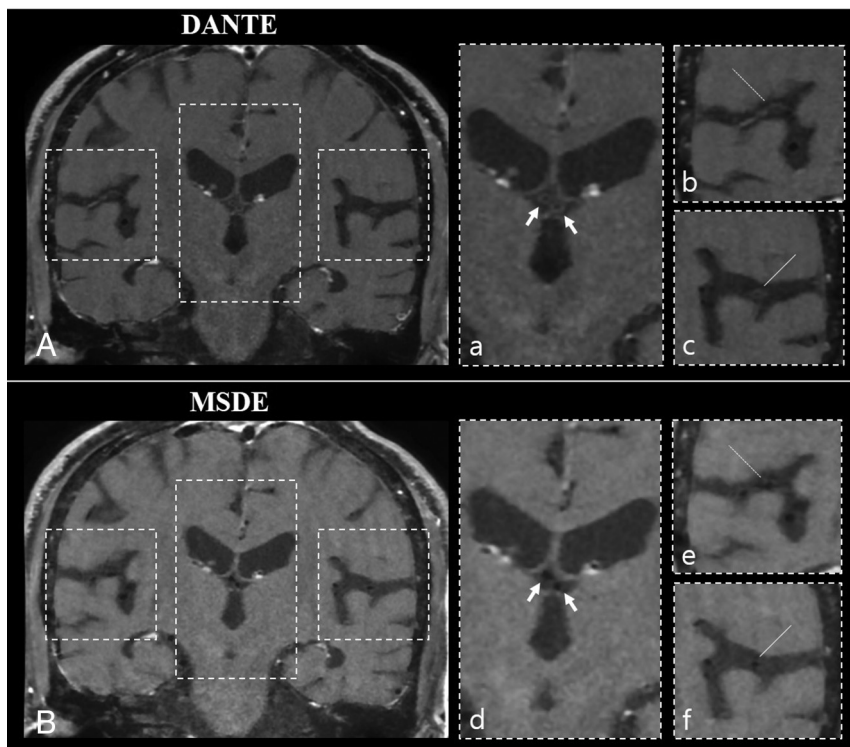


FIG 3. The detailed view of CE 3D-T1-FSE with DANTE (A) and with MSDE (B). The peripherally unsuppressed flow of the ICV (a, arrows), cortical vein in the right temporal sulci (b, dotted line), and the left M3 (c, solid line) on the CE 3D-T1-FSE with DANTE. However, superior blood suppression of the same point in each vessel was noted on CE 3D-T1-FSE with MSDE (d, arrows; e, dotted line; f, solid line).

Table 2: Comparison of SNR and CNR in the M1 segment of the MCA

Locations	3D-T1-FSE with MSDE	3D-T1-FSE with DANTE	P Value
SNR _{wall}	15.556	16.426	.099
SNR _{lumen}	7.880	8.356	.089
SNR _{csf}	16.950	16.728	.674
CNR _{wall-lumen}	10.082	9.408	.183
CNR _{wall-csf}	1.047	1.785	.013

Table 3: Comparison of image quality between 3D-T1-FSE with MSDE and DANTE

	3D-T1-FSE with MSDE	3D-T1-FSE with DANTE	P Value
Overall image quality	3.42	3.54	.013
Artifacts	3	3	NA
Blood suppression in cortical veins	3.30	2.74	<.001
Blood suppression in transverse sinuses	2.82	2.38	<.001

Note:—NA indicates not available.

.013). On the other hand, CE 3D-T1-FSE with MSDE had better blood-suppression ratings than with DANTE for the cortical veins (3.30 versus 2.74, $P < .001$) and transverse sinuses (2.82 versus 2.38, $P < .001$) (Table 3). The severity of artifacts in CE 3D-T1-FSE with MSDE and in CE 3D-T1-FSE with DANTE was rated 3 in all patients, indicating identical results.

DISCUSSION

In this study, we compared the BB effect of CE 3D-T1-FSE with MSDE and with DANTE. In the qualitative analysis, CE 3D-T1-FSE with MSDE had a significantly greater BB effect than CE 3D-T1-FSE with DANTE in the small intracranial arteries and even in the cerebral veins, cortical veins, internal cerebral veins, and transverse sinus. Both qualitative and quantitative analyses of the BB effect in the M1 of the MCA did not show significant differences between CE 3D-T1-FSE with MSDE and with DANTE. Thus, CE 3D-T1-FSE with MSDE may improve lesion conspicuity for pathologic enhancement of the vessel wall and intraluminal enhancing lesions in small vessels by decreasing venous contamination and suppressing signals from slow-flowing blood.

DANTE suppresses signals from both the blood and CSF using an alternative arrangement of low flip angle nonselective radiofrequency pulses with gradient pulses, causing static spin systems to fall into steady states.^{2,12,16} Signal suppression of the blood and CSF results from the failure of flowing spins to establish this steady state due to the spoiling effect.^{2,16} Previous studies that compared HR-VWI with or without DANTE reported that DANTE demonstrated an improved BB effect.^{3,16} Several previous studies comparing the BB effects of DANTE with those of MSDE reported the superiority of DANTE over MSDE,^{3,14,15,24,25} however, these were based on evaluations of the carotid artery,^{14,24} a phantom model of an aneurysm,³ or vessels of the neck or lower extremities.²⁵

Our study evaluated small-sized intracranial vessels using contrast enhancement because the CE sequence gives essential clinical information on vasculopathy. An adequate BB effect is crucial in avoiding incomplete blood flow suppression, which may mimic atherosclerotic plaque enhancement or vessel wall enhancement.

In contrast to previous phantom results,³ we found that DANTE demonstrated a lesser BB effect in the small intracranial vessels than MSDE. Cornelissen et al³ indicated that the use of preparation pulses when conducting HR-VWI improved the BB effect in an aneurysmal phantom, especially when using 3D-T1-turbo spin-echo (TSE) with DANTE compared with 3D-T1-TSE with MSDE. However, blood-

signal suppression is a delicate task that is affected not only by preparation pulses but also by the complex interactions of certain imaging parameters, such as voxel size, TR, TE, receiver bandwidth, and flow rate.^{26,27} Pravdivtseva et al²⁷ demonstrated the complicated relationships among flow rate, spatial resolution, and preparation pulses regarding blood-signal suppression in 3D-T1-TSE. In a scenario with a slow blood flow rate, a larger voxel size was efficient in suppressing the blood signals, more from the dominant intravoxel dephasing effect than the flow effect of the blood from the imaging section. However, when we used MSDE, the BB effect was similar between voxel sizes of 0.5 and 0.9 mm.^{3,27} Because the highest clinically feasible resolution is recommended in HR-VWI to minimize the partial volume effect,⁹ using preparation pulses with a high-spatial-resolution setting may help achieve a greater BB effect in a scenario with slow blood flow.

MSDE consists of block-shaped radiofrequency pulses with 90°–180°–90° flip angles and motion-sensitizing gradients, which dephase all moving blood spins before imaging, thus, suppressing signals from the blood.^{17,18} Previous studies have discussed the efficacy of MSDE in suppressing signals from the blood and CSF, with results indicating MSDE as an effective tool to delineate vessel walls.^{11,18,28,29} Because there is a substantial intraluminal signal increase after gadolinium injection, Lindenholz et al⁵ emphasized careful interpretation of slow-flow artifacts mostly induced by venous flow near the artery, which may cause misinterpretation of arterial wall enhancement. In our study, the visual scores of the BB effect, in the cortical veins as well as the ICV, were noticeably higher in CE 3D-T1-FSE with MSDE than in CE 3D-T1-FSE with DANTE (3.30 versus 2.74, $P < .001$; 3.72 versus 2.32, $P < .001$). We speculated that the basic difference in the composition of the 2 preparation pulse diagrams may account for our result, which is the CE situation.

DANTE is a low flip angle gradient-recalled acquisition in steady state sequence, which has T1-weighted contrast. Turbulence flow breaks the steady state, and its signal is suppressed. However, if the flow is slow or laminar, signal suppression becomes less. When the contrast agent is used, the blood-signal suppression effect may become less because of fast T1 recovery. On the other hand, the MSDE preparation consists of a 90° excitation pulse, two 180° refocusing pulses with each pulse sandwiched by bipolar motion-sensitizing gradients, and a –90° flip back pulse;²⁹ in other words, it has the characteristics of a spin-echo sequence with a motion-sensitized gradient like the diffusion-weighted spin-echo sequence. The fast T1 recovery of the contrast agent may have a low impact on the flow suppression of MSDE because MSDE has spin-echo-based T2-weighted contrast. Moreover, the gradient size is much larger than that of DANTE, and the large motion-sensitized gradient can suppress slow laminar flow.

In the qualitative analysis, although the overall image quality of MSDE was notable, CE 3D-T1-FSE with DANTE received a significantly higher score than CE 3D-T1-FSE with MSDE (3.54 versus 3.42, $P = .013$). Li et al¹⁴ speculated that compared with DANTE, MSDE reduces SNR due to T2 decay; however, our quantitative analysis revealed no significant differences in the SNR_{wall} and SNR_{csf} between CE 3D-T1-FSE with DANTE and with MSDE. There is a concern that the vessel wall SNR would be

decreased when using preparation pulses for 3D-T1-FSE.²⁰ Cho et al¹³ reported that preparation pulses may not be a requisite for MR imaging sequences with a long echo-train length and an appropriate TR (below 1160 ms; which enhances the differentiation of vessel walls from CSF and brain simultaneously clinically feasible acquisition time) in vessel wall imaging. However, we believe that preparation pulses, especially those of MSDE, need to be applied in the CE 3D-T1-FSE sequence because the intracranial blood flow is often slow, stagnant, or turbulent; thus, artifacts may pose problems in the interpretation of possible vessel wall pathologies,^{5,30} particularly when gadolinium shortens the T1 relaxation times of blood.

This study had several limitations. First, this was a retrospective study that included patients who underwent HR-VWI at a single center during a short time period. Therefore, we included only a limited number of patients. However, we used precisely controlled MR imaging settings for all patients with a randomized order of image acquisition to minimize potential bias, which could be magnified in a limited sample size. Nevertheless, the optimal sample size requires further validation. Second, we did not conduct quantitative analysis in the smaller vessels, A3, M3, P2 to P3, and the ICV, unlike in the M1 segment of the MCA. Due to the excessively thin walls of these vessels, the signal intensity acquired by measuring the ROI was easily altered by partial volume artifacts. As a substitute, we performed a qualitative analysis of the small-sized vessels using a 4-grade visual scoring system. Third, although image analysis of the lesion-free portion of the vessels was performed, the patients included in our study were those who satisfied the clinical indications of the HR-VWI examination, rather than healthy volunteers. In actual clinical settings, most individuals examined with HR-VWI are patients with pathologies. Hence, our cohort study might serve as a representative sample. Future studies including both healthy volunteers and patients with pathologies may clarify the optimal preparation pulse that could be widely used for HR-VWI.

CONCLUSIONS

MSDE demonstrated a preferable BB effect compared with DANTE on CE 3D-T1-FSE in the small intracranial arteries and even in the cerebral veins. Therefore, we suggest that CE 3D-T1-FSE with MSDE is a useful sequence for decreasing venous contamination and suppressing slow-flow artifacts, possibly leading to increased lesion conspicuity for pathologic enhancement of the vessel walls and intraluminal enhancing lesions.

Disclosure forms provided by the authors are available with the full text and PDF of this article at www.ajnr.org.

REFERENCES

1. Alexander MD, Yuan C, Rutman A, et al. **High-resolution intracranial vessel wall imaging: imaging beyond the lumen.** *J Neurol Neurosurg Psychiatry* 2016;87:589–97 [CrossRef Medline](#)
2. Arenillas JF, Dieleman N, Bos D. **Intracranial arterial wall imaging: techniques, clinical applicability, and future perspectives.** *Int J Stroke* 2019;14:564–73 [CrossRef Medline](#)
3. Cornelissen BM, Leemans EL, Coolen BF, et al. **Insufficient slow-flow suppression mimicking aneurysm wall enhancement in magnetic**

- resonance vessel wall imaging: a phantom study. *Neurosurg Focus* 2019;47:E19 [CrossRef Medline](#)
4. Dieleman N, van der Kolk AG, Zwanenburg JJ, et al. **Imaging intracranial vessel wall pathology with magnetic resonance imaging: current prospects and future directions.** *Circulation* 2014;130:192–201 [CrossRef Medline](#)
5. Lindenholz A, van der Kolk AG, Zwanenburg JJ, et al. **The use and pitfalls of intracranial vessel wall imaging: how we do it.** *Radiology* 2018;286:12–28 [CrossRef Medline](#)
6. Lee NJ, Chung MS, Jung SC, et al. **Comparison of high-resolution MR imaging and digital subtraction angiography for the characterization and diagnosis of intracranial artery disease.** *AJNR Am J Neuroradiol* 2016;37:2245–50 [CrossRef Medline](#)
7. Park JE, Jung SC, Lee SH, et al. **Comparison of 3D magnetic resonance imaging and digital subtraction angiography for intracranial artery stenosis.** *Eur Radiol* 2017;27:4737–46 [CrossRef Medline](#)
8. Chaganti J, Woodford H, Tomlinson S, et al. **Black blood imaging of intracranial vessel walls.** *Pract Neurol* 2020 Dec 23 [Epub ahead of print] [CrossRef Medline](#)
9. Mandell DM, Mossa-Basha M, Qiao Y, et al; Vessel Wall Imaging Study Group of the American Society of Neuroradiology. **Intracranial Vessel Wall MRI: Principles and Expert Consensus Recommendations of the American Society of Neuroradiology.** *AJNR Am J Neuroradiol* 2017;38:218–29 [CrossRef Medline](#)
10. Pacheco FT, Cruz Junior L, Padilha IG, et al. **Current uses of intracranial vessel wall imaging for clinical practice: a high-resolution MR technique recently available.** *Arq Neuropsiquiatr* 2020;78:642–50 [CrossRef Medline](#)
11. Wang J, Yarnykh VL, Yuan C. **Enhanced image quality in black-blood MRI using the improved motion-sensitized driven-equilibrium (iMSDE) sequence.** *J Magn Reson Imaging* 2010;31:1256–63 [CrossRef Medline](#)
12. Zhang L, Zhang N, Wu J, et al. **High resolution simultaneous imaging of intracranial and extracranial arterial wall with improved cerebrospinal fluid suppression.** *Magn Reson Imaging* 2017;44:65–71 [CrossRef Medline](#)
13. Cho SJ, Jung SC, Suh CH, et al. **High-resolution magnetic resonance imaging of intracranial vessel walls: comparison of 3D T1-weighted turbo spin echo with or without DANTE or iMSDE.** *PLoS One* 2019;14: e0220603 [CrossRef Medline](#)
14. Li L, Chai JT, Biasioli L, et al. **Black-blood multicontrast imaging of carotid arteries with DANTE-prepared 2D and 3D MR imaging.** *Radiology* 2014;273:560–69 [CrossRef Medline](#)
15. Matsuda T, Kimura H, Kabasawa H, et al. **Three-dimensional arterial spin labeling imaging with a DANTE preparation pulse.** *Magn Reson Imaging* 2018;49:131–37 [CrossRef Medline](#)
16. Xie Y, Yang Q, Xie G, et al. **Improved black-blood imaging using DANTE-SPACE for simultaneous carotid and intracranial vessel wall evaluation.** *Magn Reson Med* 2016;75:2286–94 [CrossRef Medline](#)
17. Obara M, Kuroda K, Wang J, et al. **Comparison between two types of improved motion-sensitized driven-equilibrium (iMSDE) for intracranial black-blood imaging at 3.0 Tesla.** *J Magn Reson Imaging* 2014;40:824–31 [CrossRef Medline](#)
18. Wang J, Yarnykh VL, Hatsukami T, et al. **Improved suppression of plaque-mimicking artifacts in black-blood carotid atherosclerosis imaging using a multislice motion-sensitized driven-equilibrium (MSDE) turbo spin-echo (TSE) sequence.** *Magn Reson Med* 2007;58:973–81 [CrossRef Medline](#)
19. Yoneyama M, Nakamura M, Takahara T, et al. **Improvement of T1 contrast in whole-brain black-blood imaging using motion-sensitized driven-equilibrium prepared 3D turbo spin echo (3D MSDE-TSE).** *Magn Reson Med Sci* 2014;13:61–65 [CrossRef Medline](#)
20. Cogswell PM, Siero JC, Lants SK, et al. **Variable impact of CSF flow suppression on quantitative 3.0T intracranial vessel wall measurements.** *J Magn Reson Imaging* 2018;48:1120–28 [CrossRef Medline](#)
21. Coolen BF, Schoormans J, Gilbert G, et al. **Double delay alternating with nutation for tailored excitation facilitates banding-free isotropic high-resolution intracranial vessel wall imaging.** *NMR Biomed* 2021;34: e4567 [CrossRef Medline](#)
22. Sannanjanja B, Zhu C, Colip CG, et al. **Image-quality assessment of 3D intracranial vessel wall MRI using DANTE or DANTE-CAIPI for blood suppression and imaging acceleration.** *AJNR Am J Neuroradiol* 2022;43:837–43 [CrossRef Medline](#)
23. Kang HJ, Lee JM, Joo I, et al. **Assessment of malignant potential in intraductal papillary mucinous neoplasms of the pancreas: comparison between multidetector CT and MR imaging with MR cholangiopancreatography.** *Radiology* 2016;279:128–39 [CrossRef Medline](#)
24. Papoutsis K, Li L, Near J, et al. **A purpose-built neck coil for black-blood DANTE-prepared carotid artery imaging at 7T.** *Magn Reson Imaging* 2017;40:53–61 [CrossRef Medline](#)
25. Su S, Ren Y, Shi C, et al. **Black-blood T2* mapping with delay alternating with nutation for tailored excitation.** *Magn Reson Imaging* 2017;40:91–97 [CrossRef Medline](#)
26. Alexander AL, Buswell HR, Sun Y, et al. **Intracranial black-blood MR angiography with high-resolution 3D fast spin echo.** *Magn Reson Med* 1998;40:298–310 [CrossRef Medline](#)
27. Pravdivtseva MS, Gaidzik F, Berg P, et al. **Pseudo-enhancement in intracranial aneurysms on black-blood MRI: effects of flow rate, spatial resolution, and additional flow suppression.** *J Magn Reson Imaging* 2021;54:888–901 [CrossRef Medline](#)
28. Kanoto M, Toyoguchi Y, Hosoya T, et al. **Visualization of the trochlear nerve in the cistern with use of high-resolution turbo spin-echo multisection motion-sensitized driven equilibrium.** *AJNR Am J Neuroradiol* 2013;34:1434–37 [CrossRef Medline](#)
29. Nagao E, Yoshiura T, Hiwatashi A, et al. **3D turbo spin-echo sequence with motion-sensitized driven-equilibrium preparation for detection of brain metastases on 3T MR imaging.** *AJNR Am J Neuroradiol* 2011;32:664–70 [CrossRef Medline](#)
30. Kalsoum E, Chabernaude Negrier A, Tuilier T, et al. **Blood flow mimicking aneurysmal wall enhancement: a diagnostic pitfall of vessel wall MRI using the postcontrast 3D turbo spin-echo MR imaging sequence.** *AJNR Am J Neuroradiol* 2018;39:1065–67 [CrossRef Medline](#)